

CHAPTER 3

Methodology

The full waveform inversion (FWI) algorithm used in this study performs on Matlab program, taking the advantage that the program computation based on matrix. Firstly, synthetic seismic data and partial derivative wave field are generated from the velocity model using AFD package developed by CREWES (CREWES, 2015). Then, the gradient of misfit function was calculated by cross-correlation between partial derivative wave field and residual data. On final step, a perturbation model was computed based on gradient of misfit function. A constant scale was estimated and applied to transform the gradient of misfit function unit to velocity model unit. In Figure 3.1 the FWI workflow used to calculate the perturbation model and update the initial model is illustrated.

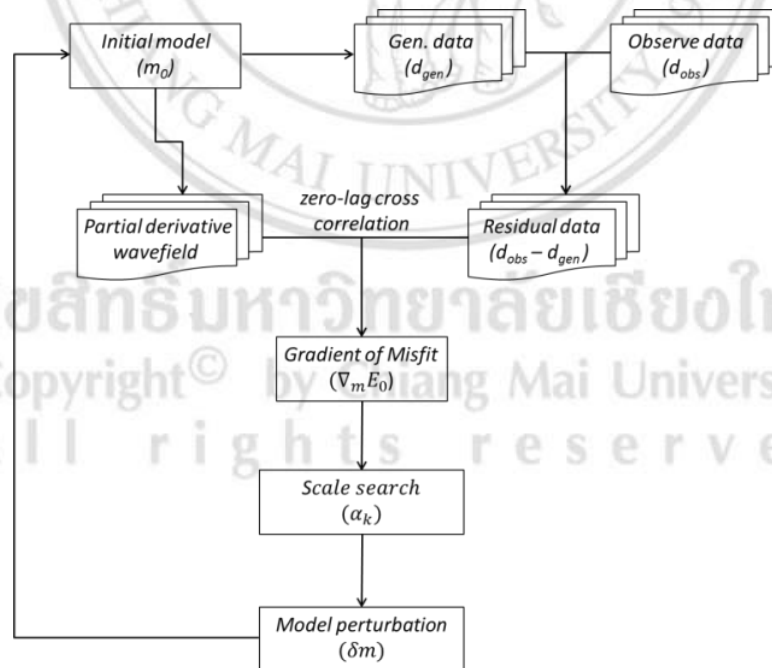


Figure 3.1 Workflow of Full Waveform Inversion (FWI)

3.1 Data generating and calculating residual data

To test FWI algorithm, first, the seismic shot records were created from true model and initial velocity model, these datasets will be therein referred to as the observed data (d_{obs}) and the generated data (d_{gen}). The synthetic data were generated based on a finite-difference constant-density solution to the 2D acoustic wave equation using MATLAB toolbox from CREWES. Several inputs information were required before running FWI algorithm, such as observed seismic data in shot domain, the initial model and survey geometry are required for creating a synthetic data as well as estimation of the wavelet of the real data.

In this study, ormsby wavelet with frequency 0 5 35 55 Hz was used as source wavelet to generate the synthetic data (both observed data and generated data). Then, the residual dataset was calculated by subtracting the generated data from the observed dataset was shown in Figure 3.4. The residual dataset was calculated shot by shot, and aiming to show missing information on the initial model.

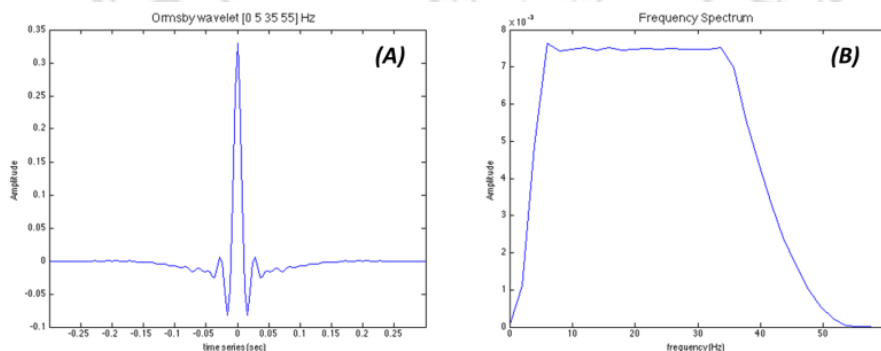


Figure 3.2 Ormsby wavelet with frequency 0 5 35 55 Hz and frequency spectrum

3.2 Effect of model boundary

By generating the synthetic seismogram from a finite velocity model, there is an effect from the impedance contrast at the model boundary, as shown in Figure 3.3. The wave field propagating through the model will reflect the energy back to receivers at this boundary. These energies are shown on the seismic record could be affect when the calculation of the gradient of misfit function. To prevent the boundary effect, it is essential to extend the velocity model before creating synthetic data. The model extension needs to be sufficient to generate the travel time reflected from these

boundaries longer than seismic records. To prevent the boundary effect in this study, 200 columns of the model were extended on each side and 300 rows were added to the bottom boundary.

3.3 Data misfit function

The misfit function was proposed to determine a degree of the difference between the true model and initial model. This function is not directly calculated from the model, but instead was estimated from phase and the amplitude difference between two synthetic datasets or the residual data by summation of the residual data square for all sample and all shot gathers. If this value is sufficiently small, it then can be considered that the initial model is close to the true model.

After model updating on each of iterative inversion, the misfit function was calculated with respect to the new model. The value was then plot and compare to each of the iterative models, to monitor the quality of the inversion. Reducing of misfit function was expected for each of the iterative inversion.

3.4 Calculating partial derivative wavefield

The partial derivative wave field was generated based on the initial velocity model using the same algorithm used to generate the initial shot gathers. As mentioned previously, the partial derivative wave field with respect to the velocity model can be interpreted as the wave field emitted at surface source, scattered by the diffraction point located at m_i and recorded by surface receivers (Operto et al., 2013). Two main steps were produced to generate the partial derivative wave field. Firstly, the virtual source term, equivalent to the wave scatter at point m_i , is estimated and recorded by surface receivers. To generate the wave field, the source point was emitted from each cell of the initial velocity model, travel though background velocity model and recorded by surface receivers. Secondly, the travel time for the wave propagated from the surface source to each cells is estimated with respect to the initial velocity model. The delay time was calculated by deriving the first arrival time of the wave initiated at the surface source and recorded by the subsurface receivers. Then the partial derivative wave fields were generated by applying a time delay to the wave travel time from the surface source to subsurface receiver to the virtual source term.

The calculation of the partial derivative wavefield with respect to model m_i is shown in Figure 3.5, which is a product of time convolution between the virtual source term (F) and the delay time that estimated from the wavefield travel through background velocity model from surface source to point m_i (E). The calculations of the partial derivative wavefield for different models were shown in Figure 3.6(A)-(E). Those wavefields were generated based on the model location (a)-(e) shown in Figure 3.4(A). The results show that different shapes of the partial derivative wavefields were obtained at different locations of the velocity model. Next, the gradient of misfit function needs to be generated as well as the partial derivative wave field, which is an essential calculation for each of the velocity cells and shot points.

As mentioned before, the partial derivative wave field is equivalent to the model of wave propagation through the model and its scatter back to surface. Sections were compared to control the quality of the partial derivative wave field. Figure 3.7-3.11 shows the partial derivative wave field from Figure 3.6 (A)-(E) overlaid with the residual data shown in Figure 3.6 (F) together with the cross-correlation result between two wave fields. It illustrates a symmetric cross- correlation with high amplitude at zero-lag, implying that the phase and time delay of these two datasets are well correlated.

3.5 Calculating gradient of misfit function

Calculation of the gradient of misfit function is equivalent to a zero-lag correlation between the residual data and the partial derivative wave field. This process detects missing information in the residual data by utilizing the partial derivative wave field. The correlation result is then transferred to the model at the location that generated the partial derivative wave field to enable the generation of the gradient of misfit function. This process is similar to migration of the residual data. The individual gradient of misfit function was calculated for each shot, and then stacked together for all individual sections to produce a global gradient of misfit function with the same size of the velocity model. The global gradient of misfit function is used to calculate the model perturbation and update the initial velocity model.

An example of the calculation of the gradient of misfit function is depicted in Figure 3.12. Different partial derivative wave fields, (C) and (D) were generated with respect to different model locations that were then correlated with the residual data in (E) and (F). The resulting zero-lag cross-correlation demonstrates high values where the partial derivative wave field is matched with the residual data, (G) and shows low values where they are different (H). The zero-lag value is then transferred to the section at the same model location used to calculate the partial derivative wave field. The partial derivative wave field is then re-calculated for the whole model to produce a full section of the gradient of misfit function, as shown in Figure 3.13. and 3.14.

3.6 Estimation of scale for model perturbation

Unfortunately, the gradient of misfit function does not provide the correct amplitude of the model perturbation. Therefore, some additional scaling (α_k) was required to estimate and convert the gradient of misfit function unit to a velocity model unit. The calculation is based on finding a constant scaling that minimises the misfit function between observed data and generated data from the new model. A set of scaling were selected, (0, 5, 10, 20, 40, 80) and used to calculate a perturbation model (δm_k) for updating the initial model. Then, several synthetic shot datasets were generated based on the new velocity model and the misfit functions were calculated according to each scaled model. A plot between scaling and the calculated misfit function was created with the parabolic curved line of fit used to search for the scaling that best minimises the misfit function, as shown in Figure 3.15.

ลิขสิทธิ์มหาวิทยาลัยเชียงใหม่
Copyright© by Chiang Mai University
All rights reserved

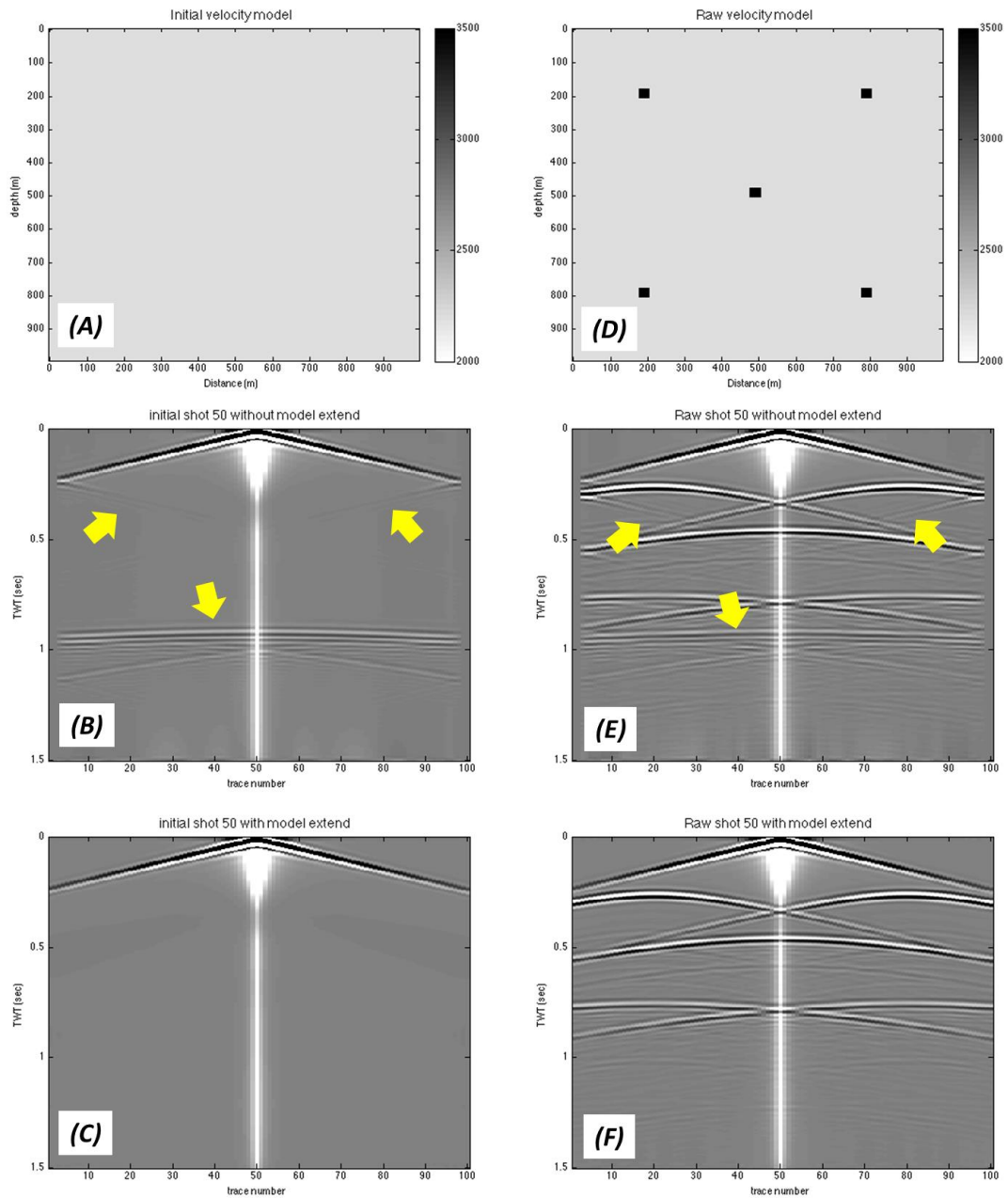


Figure 3.3 the example of shot gathers generated form model (A) and (D), shot records (B) and (E) were generated without model extension, creating reflection energy in seismic records. Shot records (C) and (F) were generated with model extension, preventing the boundary effect from shot records.

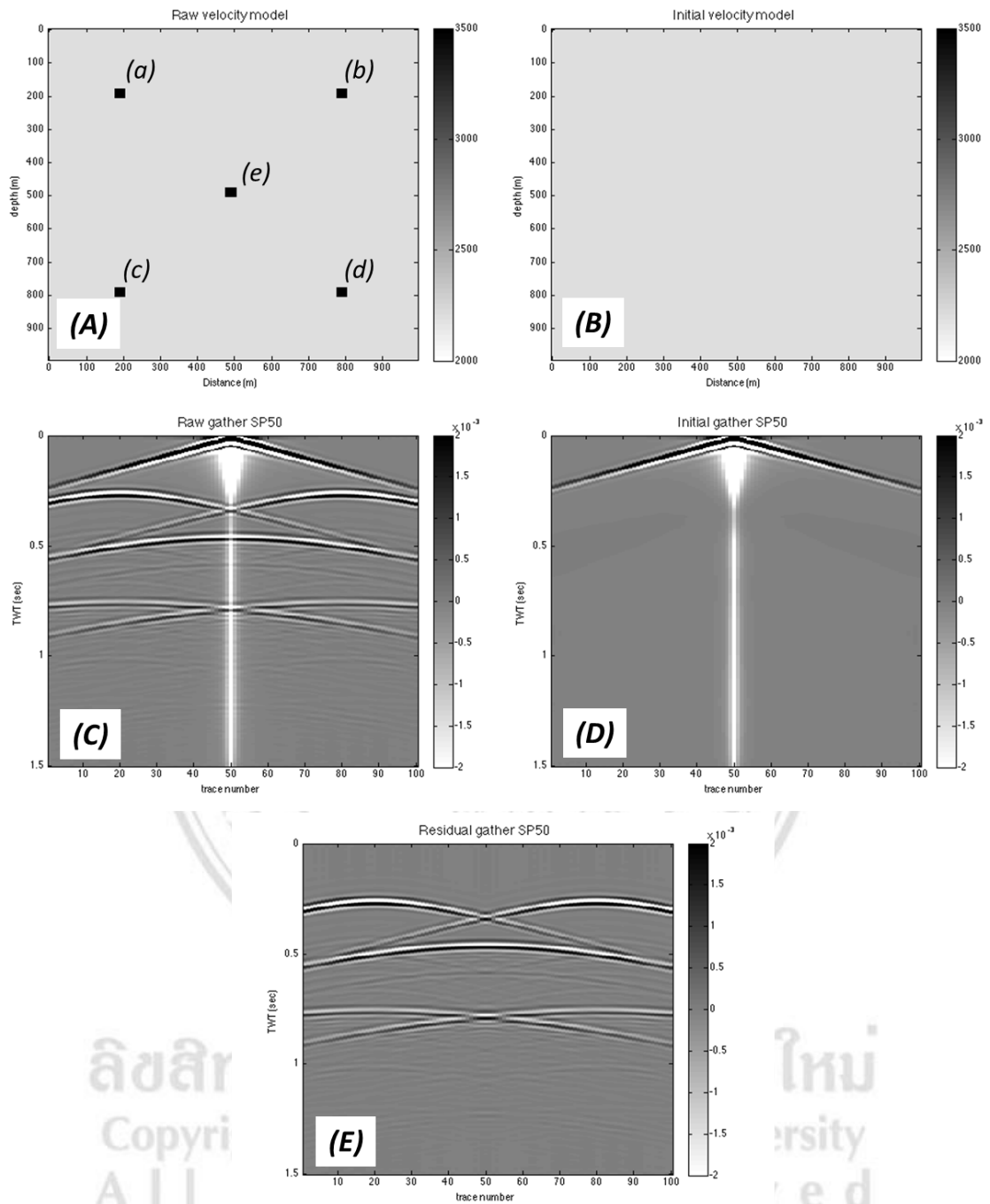


Figure 3.4 the example of synthetic shot gather, (C) and (D) generated from true velocity models (A), initial velocity model (B). The data was then subtracted to generate the residual data show on (E) which shown the missing information between (C) and (D).

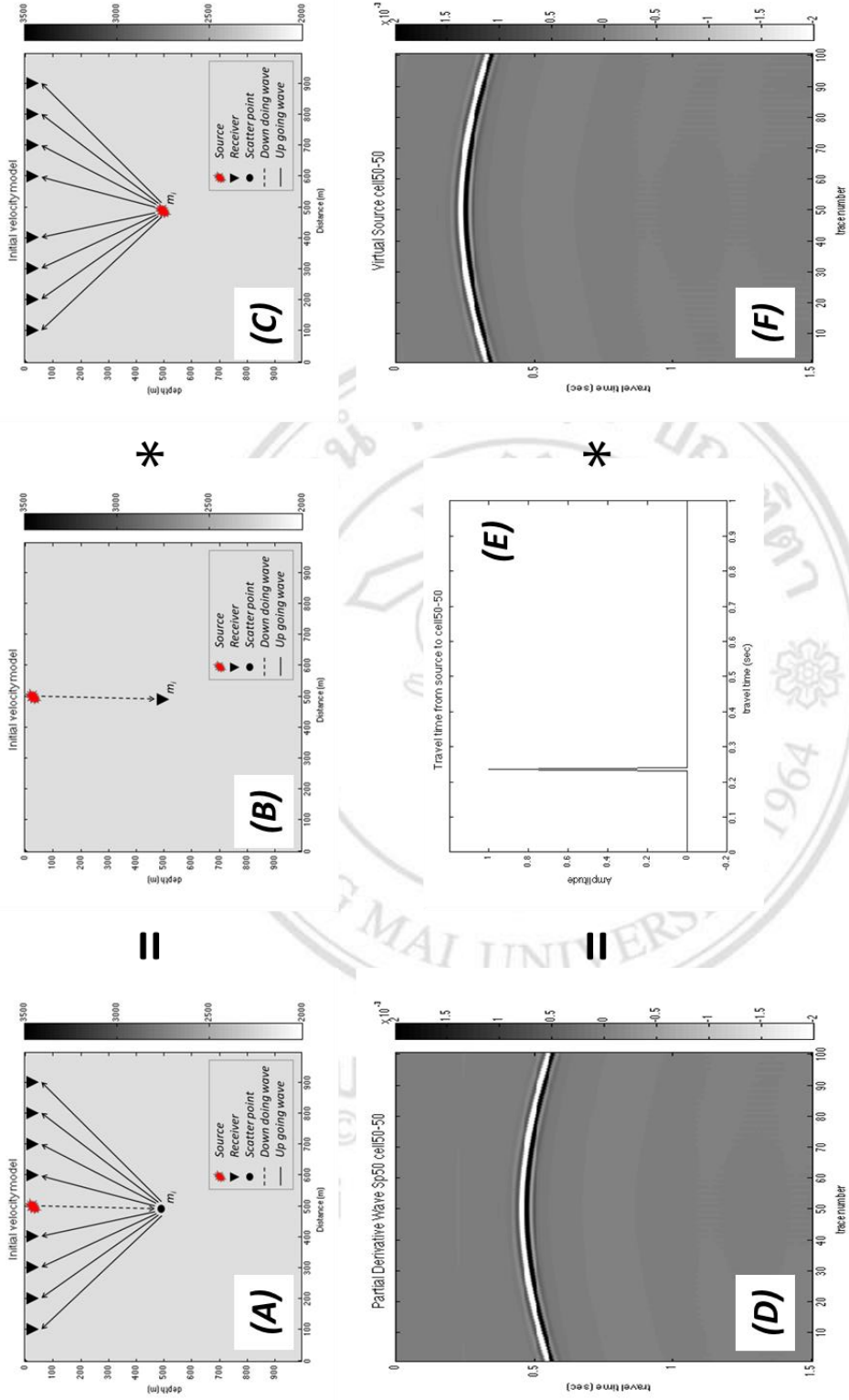


Figure 3.5 (A) and (D) represent the partial derivative wave filed with respect to model m_i . (B) and (E) show the diagram and calculated delay time for wave travel from surface to model m_i . (C) and (F) the virtual source term with respect to m_i . The partial derivative wave field showed on (D) is equivalence to time convolution be

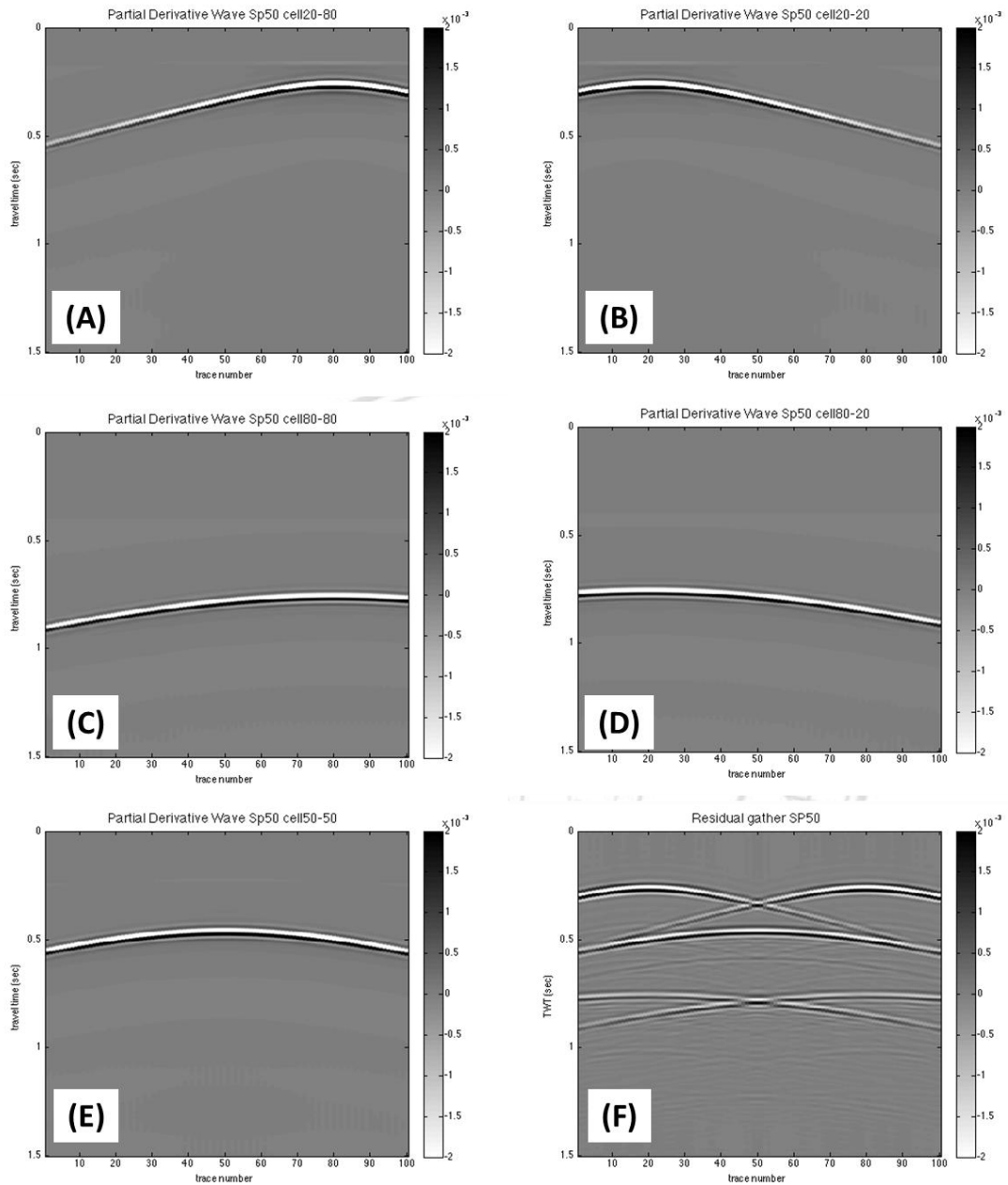


Figure 3.6 (A), (B), (C), (D), and (E) are the partial derivative wave field with respect to different model location (a), (b), (c), (d) and (e) show on Figure 3.3(A) compare to the residual data (F).

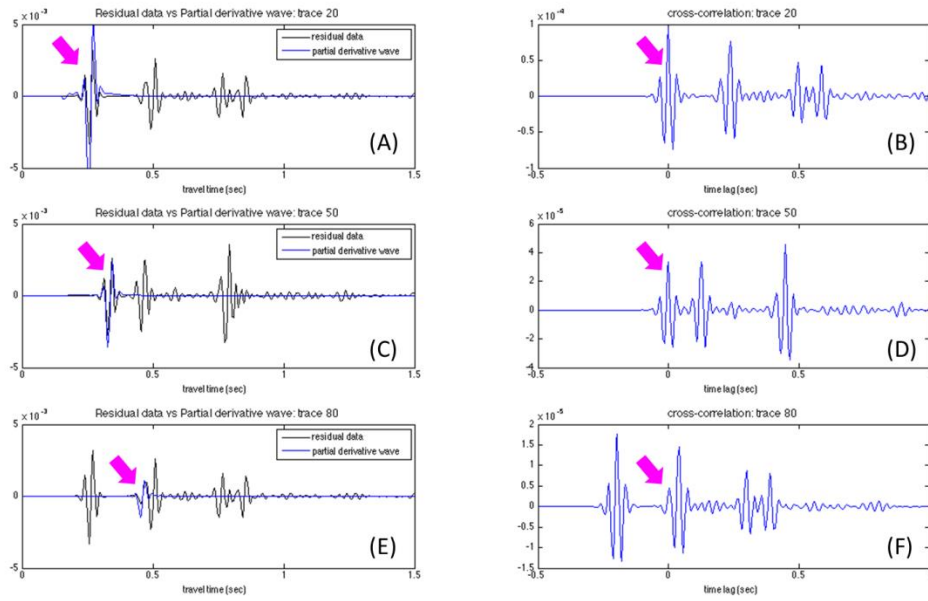


Figure 3.7 seismic trace examples (trace number 20, 50 and 80) for the partial derivative wave field show on Figure 3.5(A) overlay with the residual data show on Figure 3.5(F) together with the cross-correlation result.

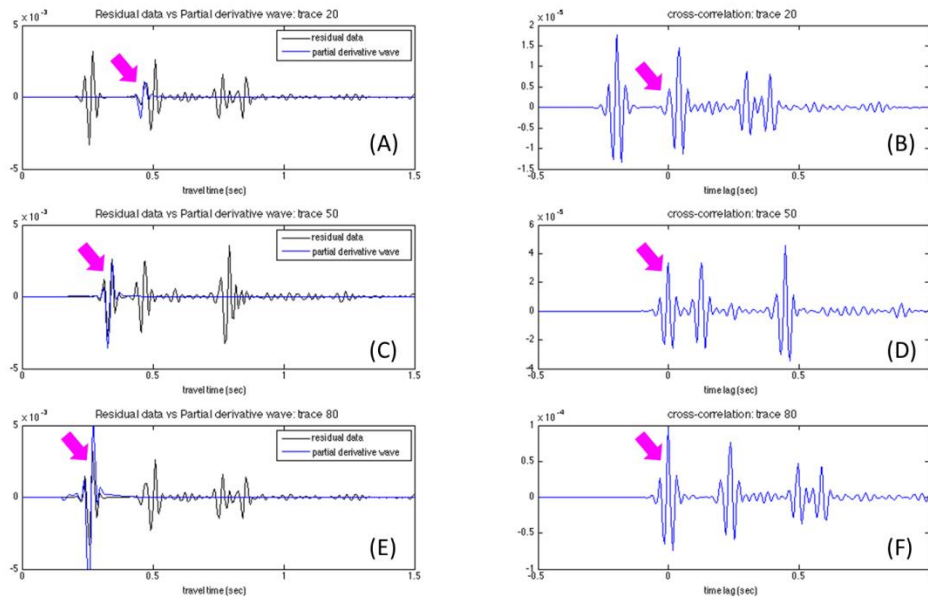


Figure 3.8 seismic trace examples (trace number 20, 50 and 80) for the partial derivative wave field show on Figure 3.5(B) overlay with the residual data show on Figure 3.5(F) together with the cross-correlation result.

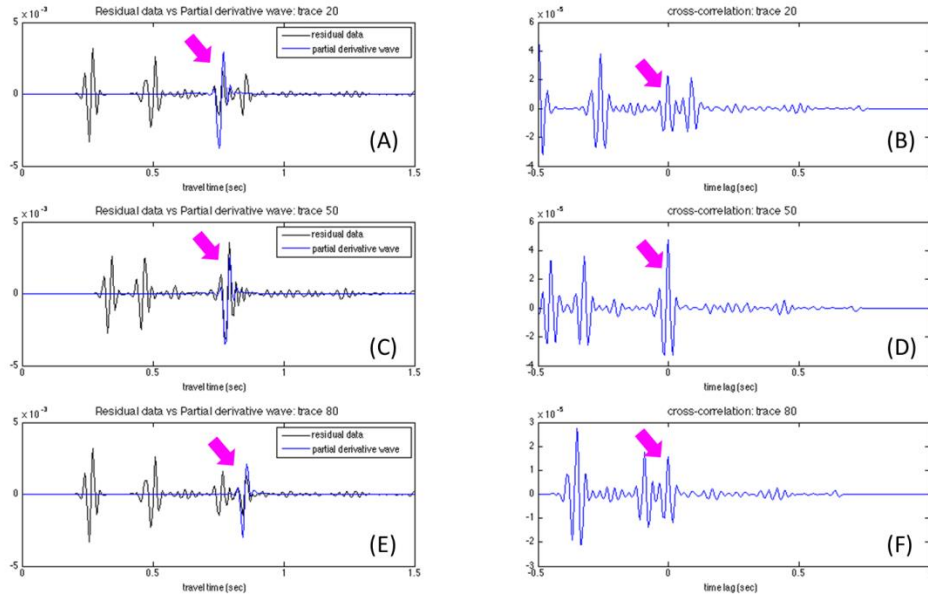


Figure 3.9 seismic trace examples (trace number 20, 50 and 80) for the partial derivative wave field show on Figure 3.5(C) overlay with the residual data show on Figure 3.5(F) together with the cross-correlation result.

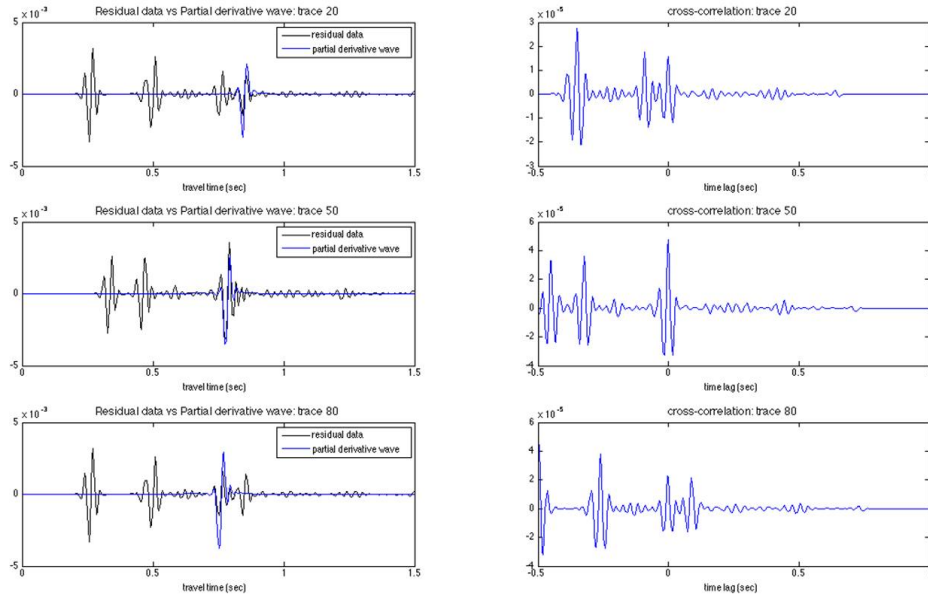


Figure 3.10 seismic trace examples (trace number 20, 50 and 80) for the partial derivative wave field show on Figure 3.5(D) overlay with the residual data show on Figure 3.5(F) together with the cross-correlation result.

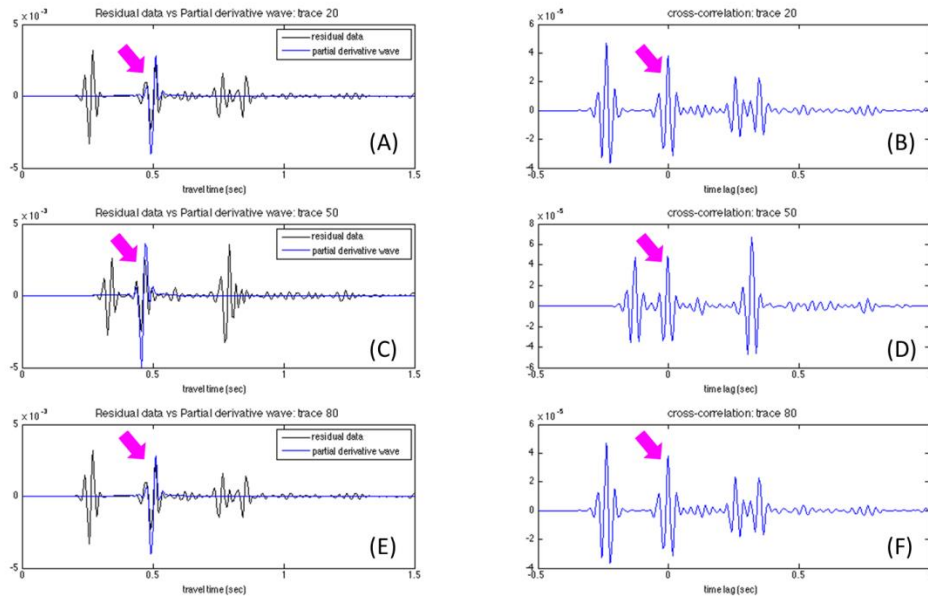


Figure 3.11 seismic trace examples (trace number 20, 50 and 80) for the partial derivative wave field show on Figure 3.5(E) overlay with the residual data show on Figure 3.5(F) together with the cross-correlation result

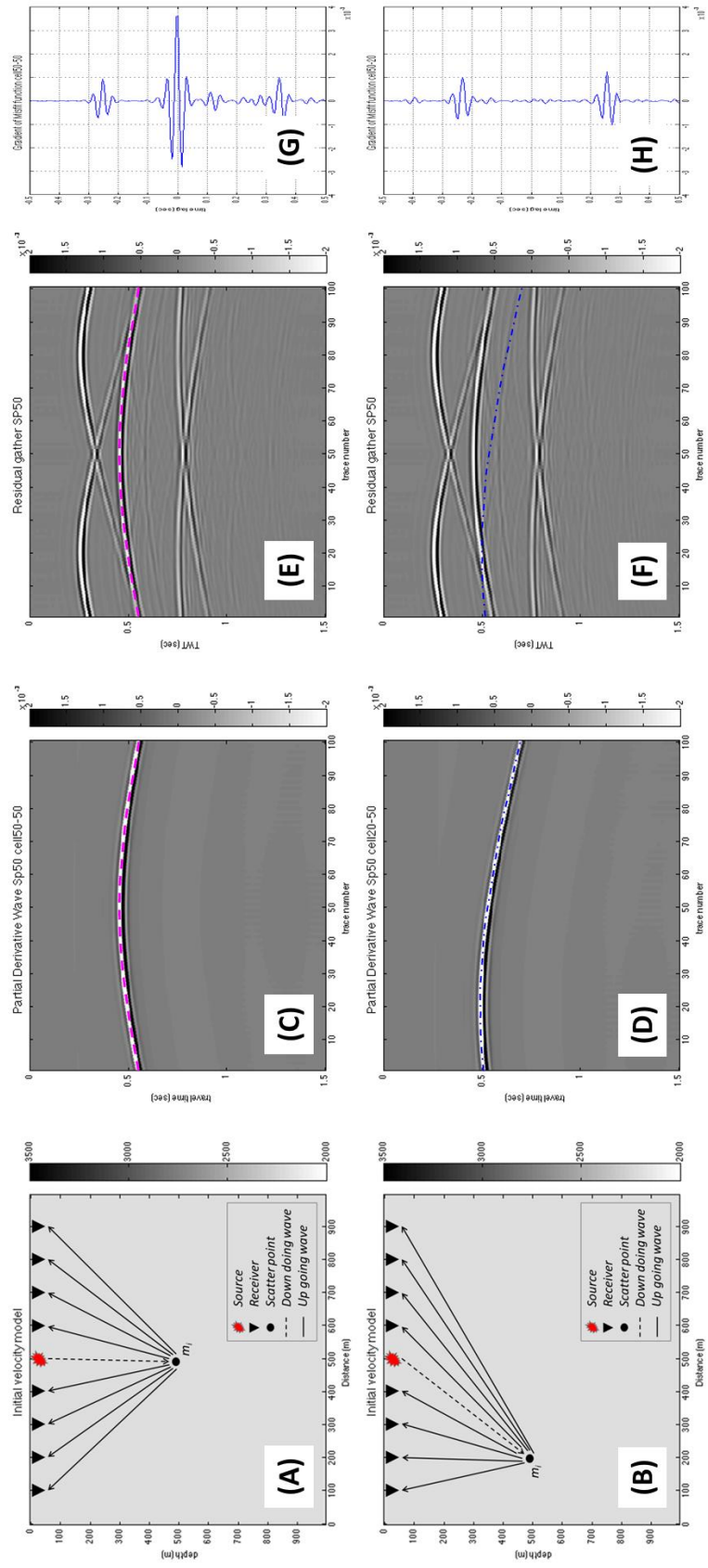


Figure 3.12 cross correlation between partial derivative wave field and residual data. (C) and (D) are the partial derivative wave field with respect to (A) and (B). (E) and (F) are the residual data from shot gather 50 overlay with partial derivative wave field show on (C) and (D). (G) and (H) show the cross-correlation result between partial derivative wave field and

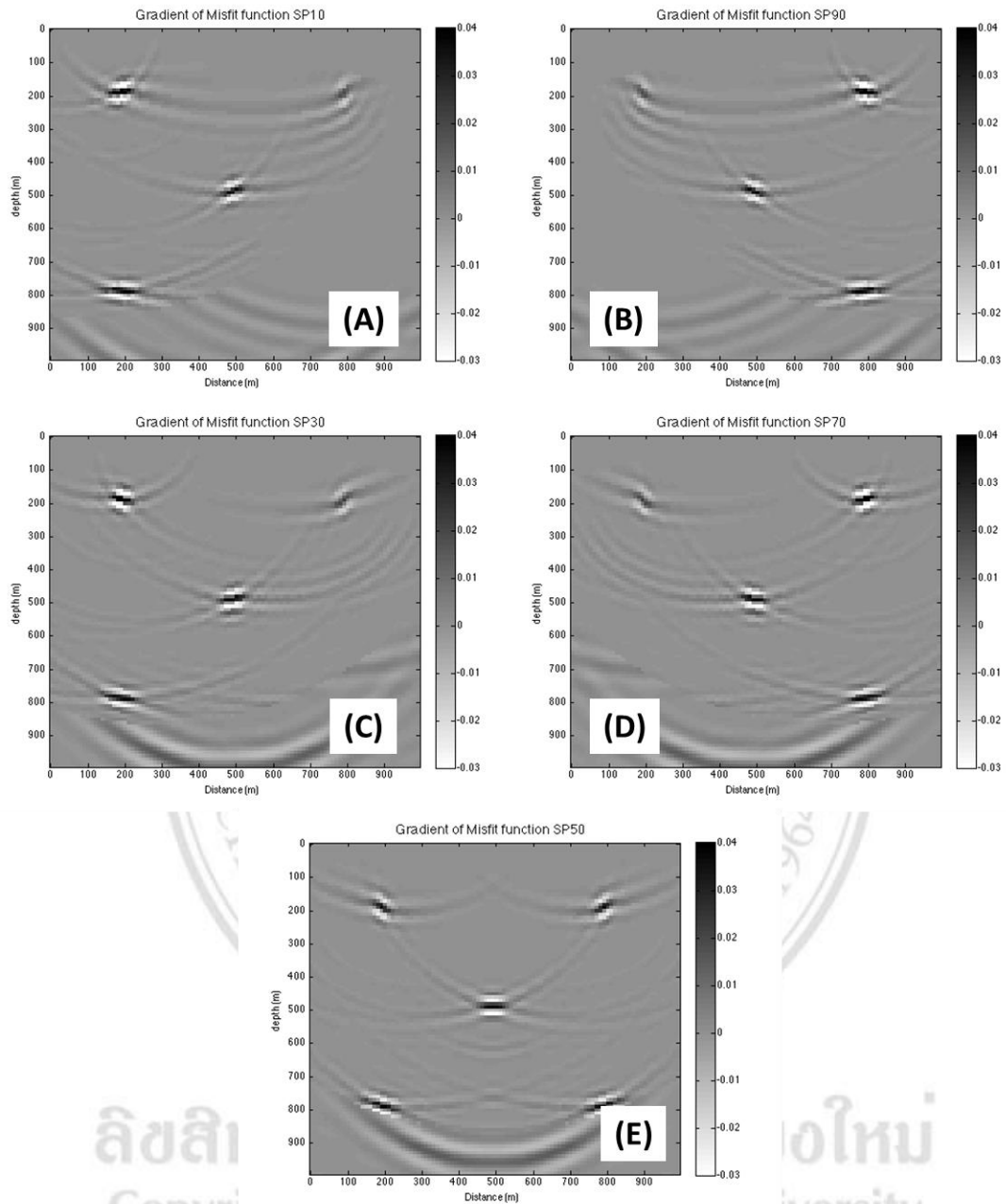


Figure 3.13 example of the individual gradient of misfit function calculated (A) shot at 100m (B) shot at 900m, (C) shot at 300m, (D) shot at 70m and (E) shot at 500m.

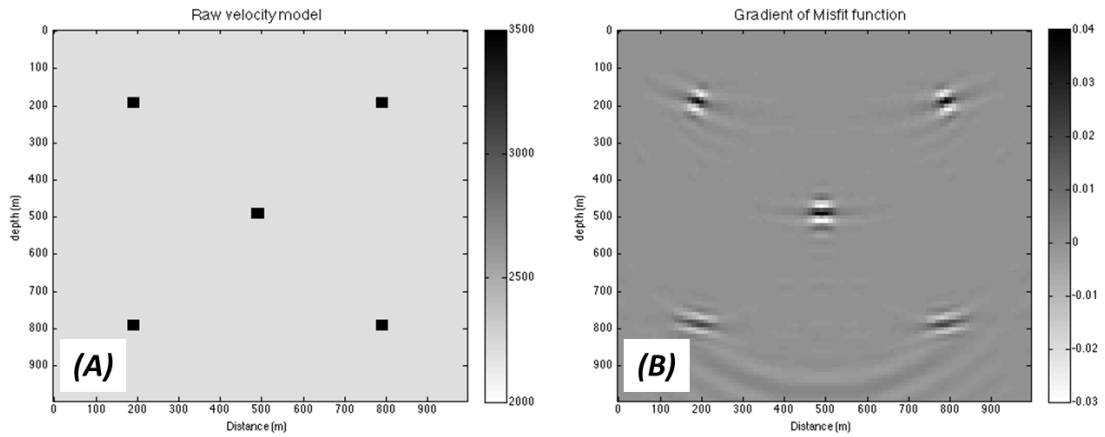


Figure 3.14 comparing between the true velocity model and the global gradient of misfit function result from the zero-lag cross-correlation between partial derivative wave field and residual data

Scale search

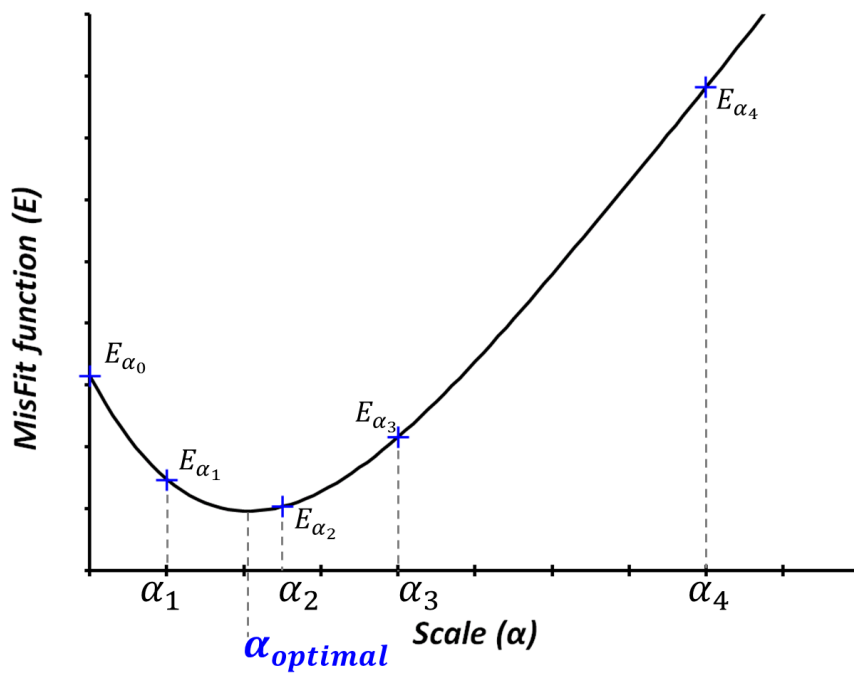


Figure 3.15 Schematic for scale search. Several points were computed to determine an optimal scaling ($\alpha_{optimal}$).